Synthesis and Characterization of Tunable Rainbow Colored Colloidal Silver Nanoparticles Using Single-Nanoparticle Plasmonic Microscopy and Spectroscopy

Tao Huang and Xiao-Hong Nancy Xu*

Department of Chemistry and Biochemistry, Old Dominion University, Norfolk, VA 23529

Keywords: nanophotonics, noble metal nanoparticles, single nanoparticle optics, plasmonic spectroscopy, silver nanoparticles

* To whom correspondence should be addressed: Email: xhxu@odu.edu; www.odu.edu/sci/xu/xu.htm; Tel/fax: (757) 683-5698

Abstract

Noble metal nanoparticles (NPs) possess size- and shape- dependent optical properties, suggesting the possibility of tuning desired optical properties of ensemble NPs at single NP resolution and underscoring the importance of probing the sizes and shapes of single NPs *in situ* and in real-time. In this study, we synthesized twelve colloids of Ag NPs. Each colloid contains various sizes and shapes of single NPs, showing rainbow colors with peak-wavelength of absorption spectra from 393 to 738 nm. We correlated the sizes and shapes of single NPs determined by high-resolution transmission electron microscopy (HRTEM) with scattering localized surface plasmon resonance (LSPR) spectra of single NPs characterized by dark-field optical microcopy and spectroscopy (DFOMS). Single spherical (2-39 nm in diameter), rod (2-47 nm in length with aspect ratios of 1.3-1.6), and triangular (4-84 nm in length with thickness of 2-27 nm) NPs show LSPR spectra (λ_{max}) at 476±5 or 533±12, 611±23, and 711±40 nm, respectively. Notably, we observed new cookie-shaped NPs, which exhibit LSPR spectra (λ_{max}) at 725±10 nm with a shoulder peak at 604±5 nm. Linear correlations of sizes of any given shape of single NPs with their LSPR spectra (λ_{max}) enable the creation of nano optical rulers (calibration curves) for identification of the sizes and shapes of single NPs in solution in real time using DFOMS, offering the feasibility of using single NPs as multicolored optical probes for study of dynamics events of interest in solutions and living organisms at nm scale in real time.

1. Introduction

Noble metal nanoparticles (e.g., Ag, Au NPs) possess size- and shape- dependent optical, electronic and catalytic properties,[1-8] inspiring a wide variety of studies and potential applications.[9-12] For example, Ag NPs exhibit localized surface plasmon resonance (LSPR) spectra (colors) that highly depend upon their sizes, shapes, and surrounding environments.[2-5] Ag NPs also show exceptionally high photostability (non-blinking and non-photodecomposition) and quantum efficiency of Rayleigh scattering that are orders of magnitude higher than fluorophors (e.g., R6G),[4, 13-16] allowing them to be imaged and characterized using dark-field optical microscopy and spectroscopy (DFOMS).[15-20]

These unique optical properties enable Ag NPs to serve as photostable and ultrasensitive optical probes and sensors for detection of single molecules and their binding kinetics, imaging of single receptors on single living cells, and probing of fluid dynamics of single embryos in real time at nanometer (nm) scale.[14-19, 21-24] Using their size-dependent LSPR spectra, sizes of single Ag NPs have been characterized at nm resolution in real time using DFOMS and utilized to probe the efflux functions and sized transformation of multidrug membrane transporters of single living cells in real time.[21-26]

Characterization of single NPs in solution offers the possibility of better understanding of interactions and ensemble optical properties of single NPs, and rational design of ensemble optical properties of Ag NPs in solution at single NP level. Current research approaches focus on fabrication or synthesis of mono-dispersed sized and shaped NPs, aiming to design and characterization of given properties of ensemble NPs.[1, 8, 27, 28] Unfortunately, none of single NPs is identical at the atomic resolution. Therefore, it is highly significant to characterize optical properties of individual NPs in solution, in order to

rationally assemble given optical properties of single NPs for creation of desired optical properties of ensemble NPs.

Notably, absorption and scattering plasmonic spectroscopy (colors) of colloidal Au and Ag NPs have been used as colorimetric assays for sensing of DNA, proteins and metal ions using native eyes,[29-31] showing the importance of design of colors (absorption and scattering optical properties) of colloidal NPs. Unfortunately, despite extensive studies, it still remains challenging to rationally design given optical properties of ensemble colloidal NPs. Even though color tunable colloids were prepared previously,[1, 8, 27, 32] none of studies characterized ensemble optical properties of colloidal Ag NPs at single NP resolution, which limits the possibility of assembly of given optical properties of single NPs to design desired optical properties of ensemble colloidal NPs.

Currently, electron microscopy (EM) is a primary means to determine the sizes and shapes of single NPs. Unfortunately, EM must be operated under high vacuum, making it unsuitable for imaging single NPs in solution and living organisms. Scanning probe microscopy (e.g., AFM or STM) has been used to charcaterize sizes and shapes of single NPs in three-dimension in solution.[7, 33] However, they cannot image free diffusion of single NPs in solution and in living organisms. These limitations demand the development of new imaging approaches.

In our previous studies, we constructed calibration curves (optical nano rulers) for nearly spherical shaped NPs in individual solution, and used optical nano rulers (size-dependent LSPR spectra of single NPs) to determine the sizes of single NPs in solution in real time using DFOMS.[34]

In this study, we developed a simple and rapid one-pot synthesis method to prepare twelve representative colloids of Ag NPs, which show tunable rainbow colors with peak wavelength (λ_{max}) of absorption spectra, ranging from 393 to 738 nm. We created nano optical rulers by correlating the sizes and shapes of single NPs determined by HRTEM with their LSPR spectra characterized by DFOMS, to determine various sizes and shapes of single NPs in each colloid. The results demonstrate the possibility of tuning the optical properties of colloids of ensemble Ag NPs using given sizes and shapes of single NPs.

2. Experimental and Simulation Section

2.1 Reagents and Supplies

Silver nitrate (≥ 99.9%), sodium borohydride (≥ 98%), sodium citrate dihydrate (≥ 99%), hydrogen peroxide (30%), and polyvinylpyrrolidone (PVP) were purchased from Sigma-Aldrich, and used as received. All solutions were prepared using nanopure de-ionized (DI) water (Barnstead).

2.2 Synthesis and Characterization of Ag NPs

Sodium citrate (3.68 mL, 30 mM), PVP (3.68 mL, 2% w/w), and H_2O_2 (120 μL, 30% w/w) were added into the freshly prepared $AgNO_3$ (43 mL, 0.11 mM in nanopure DI water) under stirring. We prepared twelve of such a mixture simultaneously. After 3 min, 100 mM $NaBH_4$ of 150, 160, 170, 180, 200, 220, 250, 280, 300, 330, 360, and 500 μL was added into each mixture, to synthesize twelve colloids of Ag NPs (Figure 1), which show light yellow, yellow, light orange, orange red, red, dark red, purple, purple violet, violet, blue, light blue, and green, respectively. Each mixture was stirred for 3 h, and filtered using 0.2 μm membrane filters, and stored in dark at 4 ^{0}C until use. The absorption and scattering plasmonic properties of Ag NPs in each colloid were characterized using UV-vis

absorption spectroscopy (Hitachi U2010). The sizes and shapes of single Ag NPs were characterized using HRTEM (FEI Tecnai G2 F30 FEG).

Optical images and LSPR spectra of single Ag NPs (Figures 2 and 3) were acquired in a micro-chamber using our DFOMS, equipped with CCD camera and Nuance Multispectral Imaging Systems (CRI), as we described previously.[12, 21-23, 34-36] Our dark-field optical microscope was equipped with a dark-field condenser (Oil 1.43-1.20, Nikon), a microscope illuminator (Halogen lamp, 100W), and a 100x objective (Nikon Plan fluor 100x oil, iris, SL. N.A. 0.5-1.3, W.D. 0.20 mm), offering the depth of field (focus) of 190 nm. Notably, the design of dark-field optical microcopy only allows scattering intensity of objects (e.g., NPs) on the focal plane to be collected by the microscope objective and recorded by detectors (e.g., CCD). Therefore, unlike those measured by UV-vis absorption spectroscopy, the LSPR spectra of single NPs acquired by DFOMS represent the scattering of single NPs, but not the absorption of single NPs.

2.3 Simulation of LSPR Spectra of Single Ag NPs

LSPR spectra of single Ag NPs were calculated using discrete dipole approximation (DDA) method and an open source Fortran-90 code, DDSCAT 7.0, developed by Draine and Flatau.[37, 38] We used wavelength dependent dielectric constants of Ag (n = 0.209-0.143, for wavelengths of 350-800 nm)[39] and the refractive index of water (1.33).[40, 41] The inter-dipole separation distance as 1 nm was set to build the cubic lattice of polarized points (dipoles) for each NP. The effective radius of each NP in Figure 6A-D was calculated as 10.1, 12.1, 9.2, and 20.8 nm, respectively. We selected bi-conjugate gradient with stabilization (PBCGS2) and general prime factor algorithm fast Fourier transform (GPFA FFT) as the iteration algorithm and the FFT algorithm, respectively. We set the angular

resolution of 0.5 and the iteration error tolerance of 10^{-5} for all calculations, as we described previously.[7]

2.4 Data Analysis and Statistics

We characterized sizes and shapes of single NPs using HRTEM, and LSPR spectra of single NPs using DFOMS. For each measurement, a minimal of 100 Ag NPs were imaged and characterized for each sample. The measurement was repeated at least three times. Therefore, a minimal of 300 Ag NPs was studied for each sample, allowing us to gain sufficient statistics for probing of size- and shape- dependent LSPR spectra of single NPs that represent ensemble NPs at single NP resolution.

3. Results and Discussion

3.1 Synthesis and Characterization of Rainbow Colored Colloidal Ag NPs

We have developed a simple and rapid one-pot synthesis method to generate twelve colloids of Ag NPs, which show rainbow colors, ranging from violet to red (Figure 1A). In this one-pot synthesis method, we utilized citrate as capping groups to stabilize the NPs and PVP to control the formation of shapes of NPs.[32] By controlling various amounts of $NaBH_4$ in the same mixture of $AgNO_3$, sodium citrate, PVP, and H_2O_2 solution,[27, 32, 42] we generated various sizes and shapes of Ag NPs in each colloid, as described in experimental section. $NaBH_4$ serves as reducing agent for synthesis of the colloidal Ag NPs. As $NaBH_4$ was added into the mixture, it rapidly reduced Ag^+ to Ag, which acts as nucleation precursors. As $NaBH_4$ concentration increases, the amount of nucleation precursors increases. Notably, the nucleation of precursors (Ag) proceeds as described by LaMer model.[43, 44] Therefore, the shapes of the Ag NPs depend upon precursor concentration, which can be tuned by the amount of $NaBH_4$.

Absorption spectra of colloids of Ag NPs in Figure 1A show peak wavelengths ranging from 393 to 738 nm, as shown in Figure 1B. For the colloid with light yellow and light orange (Figure 1a, c), single peak wavelength of absorption spectra at 383 and 427 nm was observed, respectively. All other colloids (Figure 1b, d-l) show a primary peak at 405, 461, 502, 518, 536, 552, 571, 606, 646, and 738 nm, and one or two shoulder peaks at 526, 364, 382, 422 with 342, 430 with 340, 418 with 340, 414 with 340, 416 with 338, 334, 450 with 336, and 420 with 330 nm, respectively.

3.2 Characterization of Sizes, Shapes and LSPR spectra of Single Ag NPs

To study the interesting ensemble absorption plasmonic properties of colloidal Ag NPs in Figure 1, we characterized the sizes and shapes of single NPs using HRTEM, and LSPR spectra of single colloidal NPs using DFOMS. Minimal of 300 representative individual NPs in each colloids were characterized to gain sufficient statistics that represent properties of ensemble NPs at single NP resolution. Representative HRTEM and DFOMS images of single NPs for colloidal Ag NPs in Figure 2 show that every colloid contains various sizes or shapes of single NPs. For instance, the images in Figure 2a show nearly spherical shapes in (A), spherical and rod NPs in (B), spherical, rod and triangular NPs in (C-K), and spherical, rod and cookie-like NPs in (L). Plasmonic colors of single NPs in Figure 2b show violet and cyan NPs in (A), violet, cyan and light green in (B), blue, green and yellow in (C-D), blue, green, yellow, and orange in (E-F), green, yellow, orange, and red in (G-L).

Histograms of distributions of sizes and peak wavelengths (λ_{max}) of scattering LSPR spectra of single NPs, acquired from 20 images similar to the ones in Figure 2, are shown in Figure 3. Notably, aspect ratios of rods are 1.3-1.6, and the length-to-thickness ratios of

triangular NPs are 1.7-2.5. These narrow distributions of the ratios allow us to use the lengths of the rods and lengths of triangular or cookie NPs as sizes of single NPs in the histograms. The λ_{max} of scattering LSPR spectra of single NPs at 476 ± 5, 533 ± 12, 611 ± 23, and 711 ± 40 nm are blue, green, yellow, and red NPs, respectively.

The results in Figures 2 and 3 are summarized in Tables 1 and 2. It show that: 100 of spherical NPs with average diameters of 2.6 ± 0.8 nm, which exhibits 97% of blue and 3% of green NPs in (A); 95.8% of spherical NPs with average diameters of 4.6 ± 1.1 nm and 4.2% of rod with average width and length of 3.5 ± 1.3 and 5.0 ± 2.6 nm, respectively, in (B), which shows 91.3 % of blue and 8.7% green NPs. In (C), we observed 92.4% of spherical NPs with average diameters of 9.5 ± 3.2 nm, 6.7% of rod with average width and length of 9.4 ± 3.7 and 12.1 ± 4.1 nm, and 0.9 % of triangular NPs with length and height (thickness) of 5.6 ± 1.5 and 2.9 ± 1.2 nm, which shows 76.8 % of blue and 23.2% green NPs. In (D), we observed 91.2% of spherical NPs with average diameters of 10.0 ± 3.8 nm, 7.9% of rod with average width and length of 10.5 ± 3.9 and 13.5 ± 4.2 nm, and 0.9 % of triangular NPs with length and height of 6.1 ± 1.9 and 3.5 ± 1.5 nm, which shows 31.5 % of blue and 68.5% green NPs.

In (E), we observed 59.7% of spherical NPs with average diameters of 16.1 ± 5.4 nm, 39.1% of rod with average width and length of 11.3 ± 5.2 and 15.4 ± 5.8 nm, and 1.3 % of triangular NPs with length and height of 9.5 ± 3.2 and 5.1 ± 1.8 nm, which shows 5.6 % of blue, 62.5% green, and 31.9% of yellow NPs. In (F), we found 52.5% of spherical NPs with average diameters of 18.0 ± 6.7 nm, 45.8% of rod with average width and length of 12.6 ± 5.3 and 16.5 ± 5.8 nm, and 1.7 % of triangular NPs with length and height of 21.4 ±

9.5 and 11.3 ± 2.5 nm, which shows 5.4 % of blue, 59.4% green, and 35.2% of yellow NPs.

In (G), we observed 54.1% of spherical NPs with average diameters of 16.7 ± 5.6 nm, 37.1% of rod with average width and length of 15.5 ± 4.8 and 23.1 ± 5.0 nm, and 8.8 % of triangular NPs with length and height of 23.1 ± 10.3 and 11.5 ± 2.2 nm, which shows 5.1 % of blue, 52.0% green NPs, 33.6% of yellow, and 9.3% of red NPs. In (H), we observed 46.4% of spherical NPs with average diameters of 17.1 ± 6.2 nm, 41.0% of rod with average width and length of 16.2 ± 4.8 and 25.5 ± 5.2 nm, and 12.5 % of triangular NPs with length and height of 25.5 ± 11.1 and 11.6 ± 2.6 nm, which shows 2.5 % of blue, 42.7% green, 34.4% of yellow, and 20.3% of red NPs. In (I), we observed 40.9% of spherical NPs with average diameters of 19.0 ± 5.9 nm, 44.4% of rod with average width and length of 17.2 ± 5.8 and 26.2 ± 6.2 nm, and 14.8 % of triangular NPs with length and height of 42.7 ± 21.6 and 18.2 ± 3.2 nm, which shows 4.6 % of blue, 40.2% green, 20.8% of yellow, and 34.4% of red NPs.

In (J), we found 40.2% of spherical NPs with average diameters of 20.3 ± 7.2 nm, 44.7% of rod with average width and length of 19.3 ± 6.3 and 26.6 ± 6.6 nm, and 15.2 % of triangular NPs with length and height of 54.7 ± 26.3 and 22.5 ± 4.3 nm, which shows 1.2 % of blue, 40.8% green, 15.2% of yellow, and 42.84% of red NPs. In (K), we found 35.4% of spherical NPs with average diameters of 27.0 ± 9.7 nm, 49.0% of rod with average width and length of 20.5 ± 6.6 and 29.4 ± 6.9 nm, and 15.6 % of triangular NPs with length and height of 56.8.7 ± 27.5 and 22.7 ± 4.5 nm, which shows 1.6 % of blue, 15.4% green, 3.7% of yellow, and 78.7% of red NPs.

In (L), we did not observe triangular NPs, instead of cookie shaped NPs. We found 50.7% of spherical NPs with average diameters of 29.1 ± 9.5 nm, 13.0% of rod with average width and length of 30.1 ± 9.5 and 37.2 ± 9.8 nm, and 36.2 % of cookie NPs with length of 55.3 ± 11.5 nm, which shows 2.2 % of blue, 15.4% green NPs, 3.7% of yellow, and 78.7% of red NPs.

Taken together, the sizes of spherical NPs increase and the percentage of spherical NPs decreases from colloids (A) to (L), while the sizes of rod and triangular NPs and their amounts increase. By varying the shapes (sphere, rod, triangle, and cookie) and sizes of single NPs and their amounts in the aqueous solution, we tuned the ensemble optical properties of colloidal NPs at single NP level.

By analyzing the colloidal NPs at the single NP resolution, we found that the red-shift of peak wavelengths of absorption spectra from 393 to 738 nm in Figure 1A:a-l is most likely attributable to size increase of NPs. The shoulder peaks observed in Figure 1B:b-l are attributable to the presence of rod, triangular and cookie NPs. The broad week shoulder peaks at 414-450 nm and small but sharp shoulder peaks at 330-380 nm are attributable to in-plane and out-plane quadrupole plamon resonances, which are generated by oscillating electrons between shaper edges of NPs, respectively.[2] The full-width-of-half-maximum (FWHM) of absorption spectra of colloidal Ag NPs in Figure 1B increases, as the distributions of sizes and shapes of single NPs increase (Figure 3 and Table 1).

Notably, we have synthesized a new shaped (cookie-like) NPs, which have not yet been reported previously, even though various shapes of Ag NPs, such as cube,[45] icosahedra,[42] triangle,[46] hexagon, disk,[32] rod, belt, frame,[27, 45] and shell,[45] have been reported previously.[8] The cookie shaped NPs are nano-clusters. Each cluster includes a spherical

shape NP with diameters of ~ 20 nm that is surrounded with 3-4 small NPs attached on its surface. These small NPs are spherical or polygon shapes with diameters of ~ 5 nm, and evenly distributed on the surface of a central NP. Such interesting structures would offer great opportunities to study the enhanced effects of electromagnetic fields (e.g., SERS) within a sub-nanometer gap between NPs in the clusters. Works are in progression for further exploring optical properties and potential applications of cookie shaped NPs.

3.3 Correlation of LSPR Spectra of Single Ag NPs with Their Shapes

To study the shape-dependent LSPR spectra of single Ag NPs and explore the possibility of determining the shapes of single NPs using their LSPR spectra via DFOMS, we correlated histograms of size distributions of single spherical, rod and triangular NPs measured by HRTEM with histograms of color distributions (λ_{max} of LSPR spectra) of single blue, green, yellow, and red NPs acquired by DFOMS for each colloid (Figure 4). Notably, the λ_{max} of LSPR spectra of single NPs at 476 ± 5, 533 ± 12, 611 ± 23, and 711 ± 40 nm represent single blue, green, yellow, and red NPs, respectively. The results in Figure 4 show an excellent correlation of percentage of spherical, rod and triangular NPs with that of blue and green, yellow, and red NPs, for each colloid, respectively.

Good correlations of spherical shaped NPs with plasmonic blue and green NPs were found for each of 12 colloids with 12% variation for colloid (f) and less than 8% variation for all other colloids, as shown in Figure 4A. The better correlations of rod shaped NPs with plasmonic yellow NPs were observed with less than 8% variation for colloids that contain rod NPs (a-e, g-l), and 10% variation for colloid (f), in Figure 4B. The best correlations of triangular NPs with red NPs were observed for colloids (c-k) that contain triangular NPs with less than 2.2 % of variation.

Notably, the colloid (l) contains spherical, rod and cookie shaped NPs, but not triangular NPs. By correlating the spherical NPs with blue and green NPs, and rod NPs with yellow NPs in colloid (l), we related the percentage of cookie shaped NPs with plasmonic red NPs. This approach allows us to determine the LSPR spectra of single cookie NPs.

3.4 Creation of Nano Optical Rulers by Correlating LSPR Spectra of Same-Shaped Single Ag NPs with Their Sizes

Successful correlations of LSPR spectra of single Ag NPs with their shapes in Figure 4 enable us to determine their shapes using their LSPR spectra. The results in Figure 3 show that λ_{max} of LSPR spectra for the same shape of single NPs exhibit red-shifts as the sizes of NPs increase.

To determine the correlation of the λ_{max} of LSPR spectra of single NPs with their sizes for same shaped NPs, we plotted the λ_{max} of LSPR spectra of single spherical, rod and triangular NPs versus diameters of spherical NPs, lengths of rod NPs, and lengths of triangular NPs, respectively, as shown in Figure 5. We observed astonishing linear correlations of the λ_{max} of LSPR spectra of single spherical, rod and triangular NPs with diameters of spherical NPs, lengths of rod NPs, and lengths of triangular NPs, respectively.

Taken together, we have demonstrated the feasibility of creating nano optical rulers (calibration curves) for single spherical, rod and triangular NPs in various colloids. These new imaging calibration approaches enable the determination of sizes and shapes of multiple single NPs in solution and in living organisms in real time at nm scale rapidly and simultaneously using DFOMS. These various colloids contain the same compositions of

chemicals, excpet $NaBH_4$, which offer similar dielectrc constants in each colloid and allow us to create nano optical rulers for various colloids, instead of individual colloid, as we reported previously.[34]

3.5 Identification of Sizes and Shapes of Single Ag NPs Using DFOMS

To explore the possibility of using DFOMS to determine the sizes and shapes of single NPs via the calibration approaches in Figures 4 and 5, we acquired the LSPR spectra of single NPs using DFOMS, similar to those shown in Figure 2. We first identified the shapes of single NPs based upon the correlations of LSPR spectra of single NPs with their shapes in Figure 4. We then determined their sizes using the linear calibration curves of LSPR spectra of single NPs with their sizes for a given shape of NPs in Figure 5.

The HRTEM images of representative single NPs in Figure 6a show a spherical shaped NP with a diameter of 20.3 nm in (A), a rod shaped NP with a length and width of 29.4 and 20.5 nm in (B), a triangular NP with a length and thickness of 25.5 and 22.1 nm in (C), and a cookie-shaped NP with a length and thickness of 55 and 22.3 nm in (D), respectively. These individual NPs are identified using their LSPR spectra acquired experimentally in Figure 6b-i, which show the λ_{max} at 542, 623, 725, and 701 nm, respectively.

To further verify the successful determination of single NPs with given sizes and shapes using DFOMS, we simulated the LSPR spectra of single NPs in Figure 6a using DDA approaches, as described in experimental section. The simulated LSPR spectra of single NPs in Figure 6b-ii are in excellent agreement with those measured experimentally in Figure 6b-i. Notably, the colloid in Figure 1A:l does not contain triangular NPs, but cookie shaped NPs, which enables us to distinguish the cookie NPs from triangular NPs. If NPs

with both shapes were present in the same colloid, it might be difficult to distinguish them, because NPs with both shapes share similar LSPR spectra.

Taken together, we have demonstrated the feasibility for imaging and identification of shapes and sizes of single NPs in colloidal solutions in real time at nm scale using DFOMS. These new approaches overcome optical diffraction limit of optical microscope and possess the superior characteristics of optical microscopy for probing dynamic events of interest *in situ* and *in vivo*. Notably, the noble metal NPs exhibit superior photostability (non-photobleaching and non-blinking), enabling them to serve as optical probes for study of dynamic events of interest in solution and living organisms for desired period of time.[15, 16, 18]

One potential limitation of these imaging approaches is that one needs to characterize sizes, shapes and LSPR spectra of single NPs, and construct optical nano rulers (calibration curves) of LSPR spectra versus their sizes and shapes for new colloids, before one can determine the sizes and shapes of single NPs in the solution in real time using DFOMS.

4. Summary

In summary, we have developed a rapid simple one-pot synthesis method to produce twelve representative colloidal Ag NPs that exhibit the rainbow colors, ranging from violet to red (full visible range), with peak wavelengths of absorption spectra of 393 to 738 nm. We characterized each colloid at single NP resolution. We found that the colors of colloids are tunable by controlling the various amounts of sizes and shapes of single NPs. The colloids contain spherical, rod, triangular, and cookie shaped NPs, which show λ_{max} of

scattering LSPR spectra at 476 ± 5 (blue) and 533 ± 12 (green), 611 ± 23 (yellow), 711 ± 40 nm (red), respectively. We correlated the shapes and sizes of single NPs measured by HRTEM with their LSPR spectra (λ_{max}) acquired by DFOMS, creating optical nano rulers (calibration curves) to determine the sizes and shapes of single NPs in each colloid in real time using DFOMS. Notably, cookie shaped NPs have not yet been reported previously. These cookie shaped NPs exhibited λ_{max} of LSPR spectra similar to triangular NPs. By controlling no having them in the same colloid via synthesis, we determined single triangular or cookie shaped NPs using DFOMS. These new calibration approaches enable the identification of single Ag NPs with given sizes and shapes in colloid in real time at nm scale using DFOMS, which overcome optical diffraction limit of optical microscope and offer the feasibility of using single Ag NPs as multiple colored optical probes for study of dynamic events of interest *in situ* and *in vivo*.

Acknowledgements

This work is supported in part by NSF (NIRT: BES 0507036) and NIH (R01 GM076440). We thank CharFac of University of Minnesota (a NNIN site funded by NSF) for their assistance to characterize Ag nanoparticles using HRTEM.

References

1. I. Pastoriza-Santos and L. M. Liz-Marzan, *J. Mat. Chem.*, 2008, **18**, 1724-1737.
2. K. L. Kelly, E. Coronado, L. L. Zhao and G. C. Schatz, *J. Phys. Chem. B*, 2003, **107**, 668–677.
3. C. F. Bohren and D. R. Huffman, *Absorption and Scattering of Light by Small Particles*, Wiley, New York, 1983, pp. 287-380, and references therein.
4. U. Kreibig and M. Vollmer, *Optical Properties of Metal Clusters*, Springer, Berlin, 1995, pp. 14-123, and references therein.
5. G. Mie, *Ann. Phys.* , 1908, **25**, 377-445.
6. E. Ozbay, *Science* 2006, **311**, 189-193.
7. Y. Song, P. D. Nallathamby, T. Huang, H. Elsayled-Ali and X.-H. N. Xu, *J. Phys. Chem. C.*, 2010, **114**, 74-81.
8. Y. Xia, Y. Xiong, B. Lim and S. E. Skrabalak, *Angew Chem. Int. Ed. Engl.* , 2009, **48**, 60-103
9. C. J. Murphy, A. M. Gole, J. W. Stone, P. N. Sisco, A. M. Alkilany, E. C. Goldsmith and S. C. Baxter, *Acc. Chem. Res.*, 2008, **41**, 1721-1730.
10. T. K. Sau, A. L. Rogach, F. Jäckel, T. A. Klar and J. Feldmann, *Adv. Mater. 2010*, **22**, 1805-1825.
11. A. G. Skirtach, P. Karageorgiev, B. G. De Geest, N. Pazos-Perez, D. Braun and G. B. Sukhorukov, *Adv Mater*, 2008, **20**, 506-510.
12. X.-H. N. Xu, Y. Song and P. D. Nallathamby, in *New Frontiers in Ultrasensitive Bioanalysis: Advanced Analytical Chemistry Applications in Nanobiotechnology, Single Molecule Detection, and Single Cell Analysis*, ed. X.-H. N. Xu, Wiley, New Jersey, 2007, pp. 41-65.
13. P. K. Jain, X. Huang, I. H. El-Sayed and M. A. El-Sayed *Acc. Chem. Res.*, 2008, **41**, 1578–1586.
14. J. Yguerabide and E. E. Yguerabide, *Anal. Biochem.*, 1998, **262**, 137-156.
15. T. Huang, P. D. Nallathamby and X.-H. N. Xu, *J. Am. Chem. Soc.* , 2008, **130**, 17095-17105.
16. K. J. Lee, P. D. Nallathamby, L. M. Browning, C. J. Osgood and X.-H. N. Xu, *ACS Nano*, 2007, **1**, 133-143.

17. T. Huang, P. D. Nallathamby, D. Gillet and X.-H. N. Xu, *Anal. Chem.*, 2007, **79**, 7708-7718.
18. P. D. Nallathamby, K. J. Lee and X.-H. N. Xu, *ACS Nano*, 2008, **2**, 1371-1380.
19. S. Schultz, D. R. Smith, J. J. Mock and D. A. Schultz, *Proc. Natl. Acad. Sci. U. S. A.*, 2000, **97**, 996-1001.
20. G. H. Chan, J. Zhao, G. C. Schatz and R. P. Van Duyne, *J. Phys. Chem. C.*, 2008, **112**, 13958-13963
21. S. V. Kyriacou, W. J. Brownlow and X. H. N. Xu, *Biochemistry*, 2004, **43**, 140-147.
22. X.-H. N. Xu, W. J. Brownlow, S. V. Kyriacou, Q. Wan and J. J. Viola, *Biochemistry*, 2004, **43**, 10400-10413.
23. X.-H. N. Xu, J. Chen, R. B. Jeffers and S. V. Kyriacou, *Nano Letters*, 2002, **2**, 175-182.
24. X.-H. N. Xu and R. P. Patel, in *Encyclopedia of Nanoscience and Nanotechnology*, ed. H. S. Nalwa, American Scientific Publishers, Stevenson Ranch, CA, 2004, pp. 189-192.
25. K. J. Lee, L. M. Browning, T. Huang, F. Ding, P. D. Nallathamby and X.-H. N. Xu, *Anal. Bioanal. Chem.*, 2010, **397**, 3317-3328.
26. P. D. Nallathamby, K. J. Lee, T. Desai and X.-H. N. Xu, *Biochemistry*, 2010, **49**, 5942-5953.
27. G. S. Métraux and C. A. Mirkin, *Adv Mater*, 2005, **17**, 412-415.
28. A. J. Haes and R. P. Van Duyne, *J. Am. Chem. Soc.*, 2002, **124**, 10596-10604.
29. J. J. Storhoff, R. Elghanian, R. C. Mucic, C. A. Mirkin and R. L. Letsinger, *J. Am. Chem. Soc.*, 1998, **120**, 1959-1964.
30. J.-M. Nam, C. S. Thaxton and C. A. Mirkin, *Science* 2003, **301**, 1884-1886
31. J. Liu and Y. Lu, *Chem. Comm.* , 2007, 4872-4874.
32. S. H. Chen, Z. Y. Fan and D. L. Carroll, *J. Phys. Chem. B*, 2002, **106**, 10777-10781.
33. A. J. Haes, J. Zhao, S. Zou, C. S. Own, L. D. Marks, G. C. Schatz and R. P. Van Duyne, *J. Phys. Chem. B* 2005, **109**, 11158-11162.
34. P. D. Nallathamby, T. Huang and X.-H. N. Xu, *Nanoscale*, 2010, **2**, 1715 - 1722.
35. S. V. Kyriacou, M. E. Nowak, W. J. Brownlow and X.-H. N. Xu, *J. Biomed. Opt.*, 2002, **7**, 576-586.

36. X.-H. N. Xu, W. J. Brownlow, S. Huang and J. Chen, *Biochem. Biophys. Res. Commun.*, 2003, **305**, 79-86.
37. B. T. Draine and P. J. Flatau, *J. Opt. Soc. Am. A*, 1994, **11**, 1491-1499.
38. B. T. Draine and P. J. Flatau, *"User Guide to the Discrete Dipole Approximation Code DDSCAT 7.0",* **http://arXiv.org/abs/0809.0337v5** (2008).
39. E. D. Palik, *Handbook of Optical Constants of Solids*, Academic Press, Inc., New York, 1985, pp. 354.
40. D. K. Lynch and W. Livingston, *Color and Light in Nature*, Cambridge University Press, Cambridge, UK, 2001, pp. 109.
41. R. M. Pope and E. S. Fry, *Appl. Opt.* , 1997, **36**, 8710-8723.
42. A. Henglein and M. Giersig, *J. Phys. Chem. B*, 1999, **103**, 9533-9539.
43. V. K. LaMer and R. H. Dinegar, *J. Am. Chem. Soc.*, 1950, **72**, 4847-4854.
44. M. A. Watzky and R. G. Finke, *J. Am. Chem. Soc.*, 1997, **119**, 10382–10400.
45. Y. Sun and Y. Xia, *Anal. Chem.*, 2002, **74**, 5297-5305.
46. R. Jin, Y. Cao, C. A. Mirkin, K. L. Kelly, G. C. Schatz and J. G. Zheng, *Science*, 2001, **294**, 1901-1903.

Table 1: Summary of Sizes and Shapes of Single Ag NPs in Colloids

Colloidal Color (λ_{max}, nm)[a]	Shape								
	Sphere		Rod			Triangle		Cookie	
	%	D[b] (nm)	%	L[c] (nm) W[d] (nm)	R[e]	%	L (nm) H[f] (nm)	%	L (nm) H (nm)
a: Light yellow 393	100	2.6 ± 0.8							
b: Yellow 405	95.8	4.6 ± 1.1	4.2	5.0 ± 2.6 3.5 ± 1.3	1.4				
c: Light orange 427	92.4	9.5 ± 3.2	6.7	12.1 ± 4.1 9.4 ± 3.7	1.3	0.9	5.6 ± 1.5 2.9 ± 1.2		
d: Orange red 461	91.2	10.0 ± 3.8	7.9	13.5 ± 4.2 10.5 ± 3.9	1.3	0.9	6.1 ± 1.9 3.5 ± 1.5		
e: Red 502	59.7	16.1 ± 5.4	39.1	15.4 ± 5.8 11.3 ± 5.2	1.4	1.3	9.5 ± 3.2 5.1 ± 1.8		
f: Dark red 518	52.5	18.0 ± 6.7	46	16.5 ± 5.8 12.6 ± 5.3	1.3	1.7	21.4 ± 9.5 11.3 ± 2.5		
g: Purple 536	54.1	16.7 ± 5.6	37.1	23.1 ± 5.0 15.5 ± 4.8	1.5	8.8	23.1 ± 10.3 11.5 ± 2.2		
h: Purple violet 552	46.4	17.1 ± 6.2	41.0	25.5 ± 5.2 16.2 ± 4.8	1.6	12.5	25.5 ± 11.1 11.6 ± 2.6		
i: Violet 572	40.9	19.0 ± 5.9	44.4	26.2 ± 6.2 17.2 ± 5.8	1.5	14.8	42.7 ± 21.6 18.2 ± 3.2		
j: Blue 606	40.2	20.3 ± 7.2	44.7	26.6 ± 6.6 19.3 ± 6.3	1.4	15.2	54.7 ± 26.3 22.5 ± 4.3		
k: Light blue 646	35.4	27.0 ± 9.7	49.0	29.4 ± 6.9 20.5 ± 6.6	1.4	15.6	56.8 ± 27.5 22.7 ± 4.5		
L: Green 738	50.7	29.1 ± 9.5	13.0	37.2 ± 9.8 30.1 ± 9.5	1.2			36.2	55.3 ± 11.5 22.3 ± 5.1

λ_{max}[a]: peak wavelength of UV-vis absorption spectra of colloids;

D[b]: Average diameters of single NPs;

L[c]: Average lengths of rod or length of single triangular NPs;

W[d]: Average widths (diameters) of single rod NPs;

R[e]: Average of aspect ratios of single rod NPs;

H[f]: Average of height (thickness) of single triangular or cookie NPs

Table 2: Summary of LSPR Spectra of Single Ag NPs in Colloids

Colloidal Color (λ_{max}, nm)[a]	%	Colors (λ_{max} of Scattering LSPR Spectra) of Single NPs (nm)			
		Blue	Green	Yellow	Red
		476 ± 5	533 ± 12	611 ± 23	711 ± 40
a: Light yellow (393 nm)	%	97.0	3.0		
b: Yellow (405 nm)	%	91.3	8.7		
c: Light orange (427 nm)	%	76.8	23.2		
d: Orange red (461 nm)	%	31.5	68.5		
e: Red (502 nm)	%	5.6	62.5	31.9	
f: Dark red (518 nm)	%	5.4	59.4	35.2	
g: Purple (536 nm)	%	5.1	52.0	33.6	9.3
h: Purple violet (552 nm)	%	2.5	42.7	34.5	20.3
i: Violet (572 nm)	%	4.6	40.2	20.8	34.4
j: Blue (606 nm)	%	1.2	40.8	15.2	42.8
k: Light blue (646 nm)	%	1.6	23.7	8.9	65.8
L: Green (738 nm)	%	2.2	15.4	3.7	78.7

λ_{max}[a]: peak wavelength of UV-vis absorption spectra of colloids

Figure Captions

Figure 1: Study of absorption and scattering plasmonic optical properties of colloidal Ag NPs using UV-vis absorption spectroscopy.

(A) Photos of colloids show: (a) light yellow; (b) yellow; (c) light orange; (d) orange-red; (e) red; (f) dark red; (g) purple; (h) purple violet; (i) violet; (j) blue; (k) light blue; and (l) green colors.

(B) Normalized absorbance of UV-vis absorption spectra of the colloids of Ag NPs in (A) shows the peak wavelength (λ_{max}) with FWHM at: (a) 393 nm (64 nm); (b) 405 nm (69 nm) with a weak shoulder peak at 526 nm; (c) 427 nm (110 nm) with a weak shoulder peak at 364 nm; (d) 461 nm (192 nm) with a weak shoulder peak at 382 nm; (e) 502 nm (160 nm) with two week shoulder peaks at 422 and 342 nm; (f) 518 nm (146 nm) with two week shoulder peaks at 430 and 340 nm; (g) 536 nm (158 nm) with two shoulder peaks at 418 and 340 nm; (h) 552 nm (166 nm) with two shoulder peaks at 414 and 340 nm; (i) 572 nm (172 nm) with two shoulder peaks at 416 and 338 nm; (j) 606 nm (212 nm) with a should peak at 334 nm; (k) 646 nm (215 nm) with two shoulder peaks at 450 and 336 nm; and (l) 738 nm (130 nm) with two shoulder peaks at 420 nm (78 nm) and 330 nm.

Figure 2: Characterization of (a) sizes and shapes and (b) LSPR spectra of single Ag NPs for colloids in Figure 1, using HRTEM and DFOMS, respectively. The results are summarized in Tables 1 and 2. The scale bars in (a) are 40 and 100 nm for (A-H) and (I-L), and 10 μm in (b), respectively. Single NPs in (b) are imaged under optical diffraction limit and thereby the scale bars in (b) represents the distances among NPs, but not the sizes of NPs.

Figure 3: Study of distributions of sizes and shapes of single Ag NPs measured by HRTEM and their LSPR scattering spectra acquired by DFOMS. (a) Histograms of size distribution of single NPs; (b) Histograms of peak wavelength (λ_{max}) of LSPR spectra of single Ag NPs, for colloids of (A-L) in Figure 1. The results are summarized in Tables 1 and 2. Sizes of NPs in (a) are diameters of spherical NPs, and lengths of rod, triangular and cookie NPs. The largest cross distances between small NPs surrounding the larger central NP in cookie NPs are determined as the lengths of the cookie NPs.

Figure 4: Study of shape-dependent LSPR spectra (λ_{max}) of single NPs for colloids in Figure 1. Correlations of percentage of single (A) plasmonic blue and green NPs with spherical NPs; (B) plasmonic yellow NPs with rod NPs; and (C) plasmonic red NPs with triangular NPs. Peak wavelengths (λ_{max}) of LSPR spectra of single blue, green, yellow, and red NPs are 476 ± 5, 533 ± 12, 611 ± 23, and 711 ± 40 nm, respectively.

Figure 5: Study of size-dependent LSPR spectra (λ_{max}) of single Ag NPs for the same shaped NPs. Plots of peak wavelength (λ_{max}) of single Ag NPs versus (A) diameters of single spherical NPs; (B) lengths of single rod NPs; and (C) lengths of single triangular NPs, show high linear correlations with linear regression (R^2) of 0.95, 0,98 and 0.99, respectively.

Figure 6: Identification of sizes and shapes of single Ag NPs using DFOMS. (a) TEM images and (b): (i) experimental and (ii) DDA simulated LSPR spectra of single Ag NPs, for: (A) spherical (D = 20.3 nm): (i) $\lambda_{max, e}$ = 542 nm (FWHM = 64 nm), (ii) $\lambda_{max, c}$ = 541 nm (76 nm); (B) rod (L = 29.4 nm; W = 20.5 nm): (i) $\lambda_{max, e}$ = 623 nm (102 nm), (ii) $\lambda_{max, c}$ = 624 nm (95 nm); (C) triangular (L = 25.5 nm; H = 22.1 nm): (i) $\lambda_{max, e}$ = 725 nm (105 nm), (ii) $\lambda_{max, c}$ = 700 nm (114 nm); and cookie shaped (L = 55 nm; H = 22.3 nm): (i) $\lambda_{max, e}$ = 713 nm (119 nm), (ii) $\lambda_{max, c}$ = 701 nm (118 nm). The scale bars are 20 nm.

Figure 1

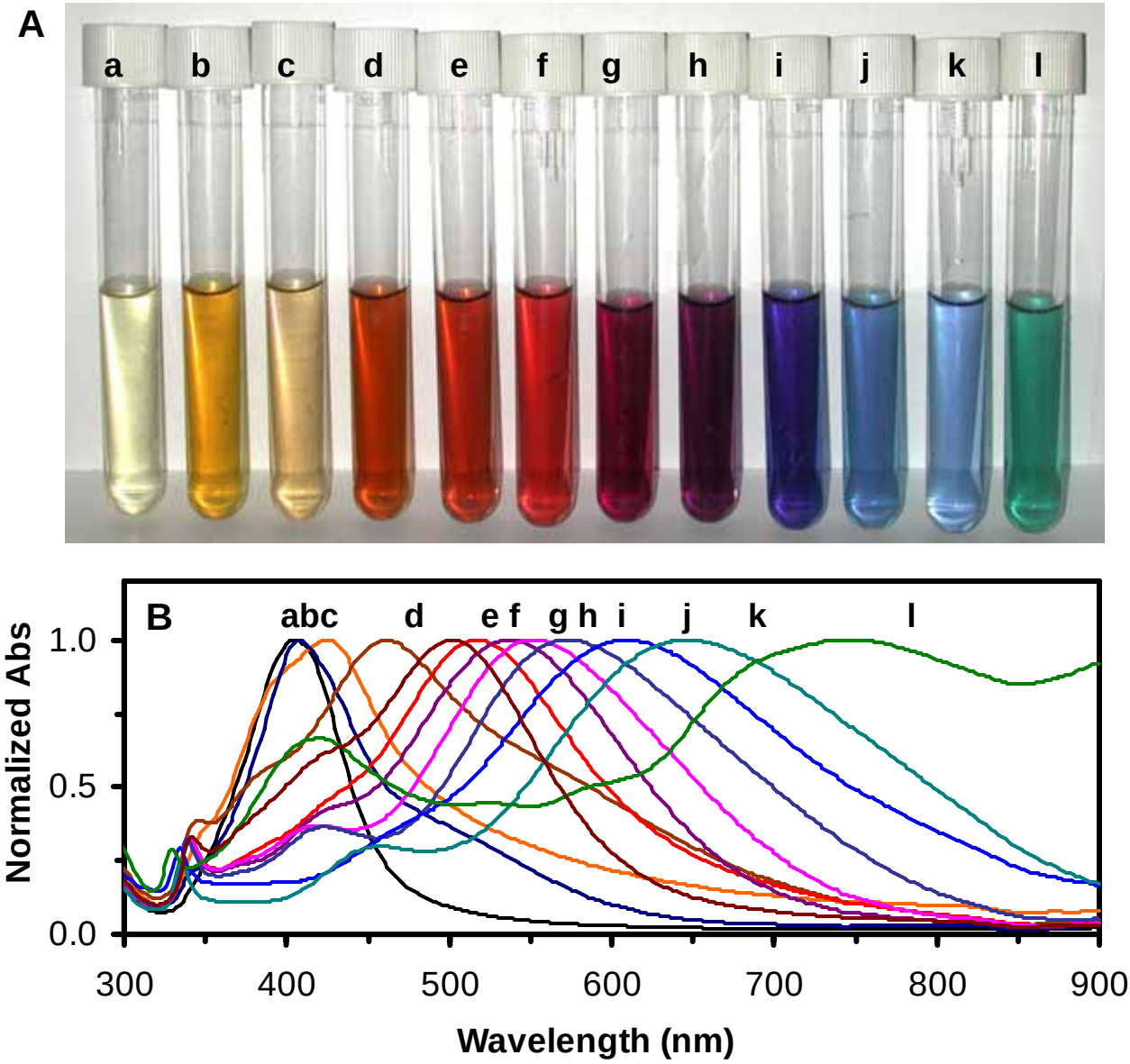
A
a
b
c
d
e
f
g
h
i
j
k
l
B
abc
d
e f
g h
i
j
k
l
Normalized Abs
1.0
0.5
0.0
300
400
500
600
700
800
900
Wavelength (nm)

Figure 2

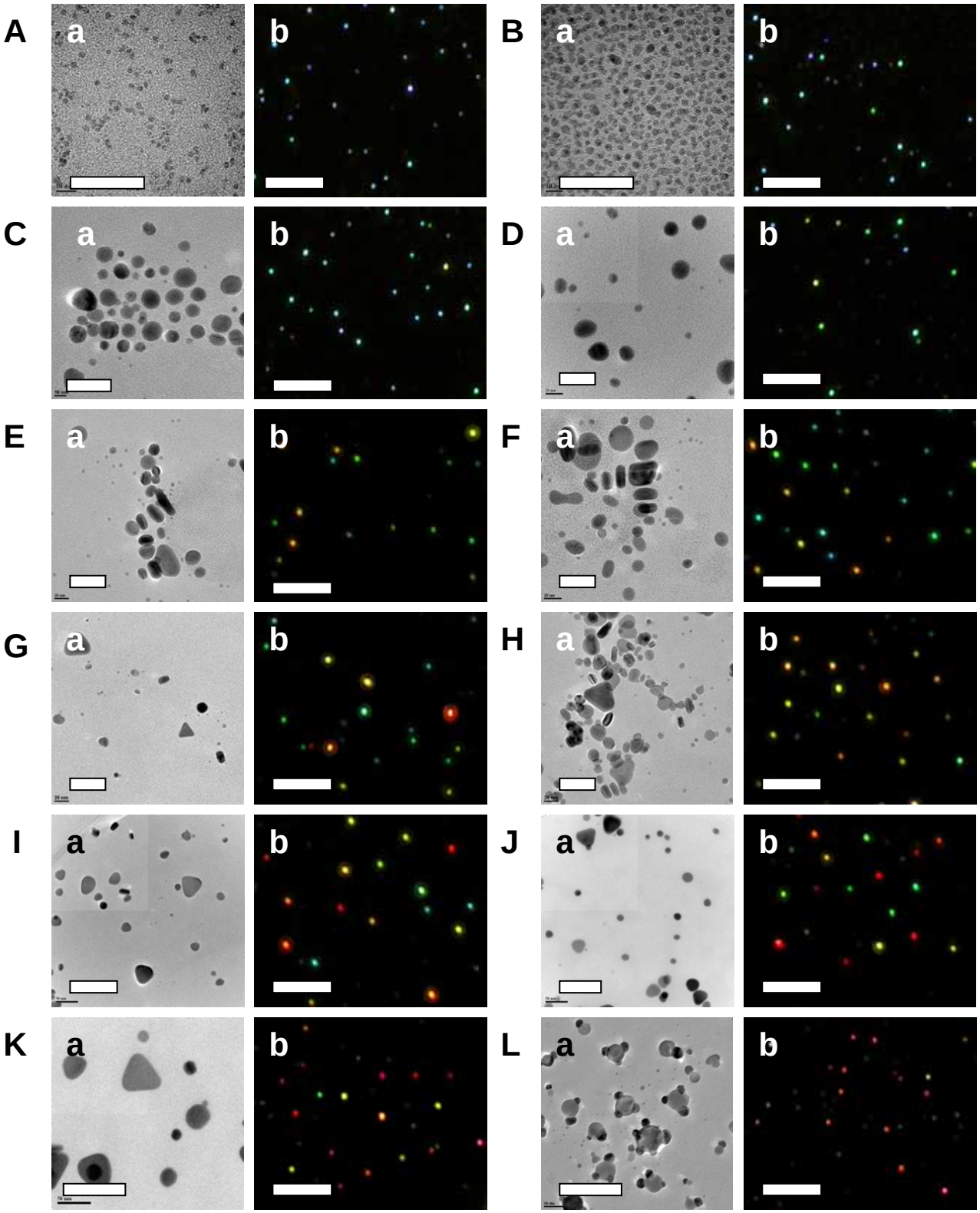

Figure 3

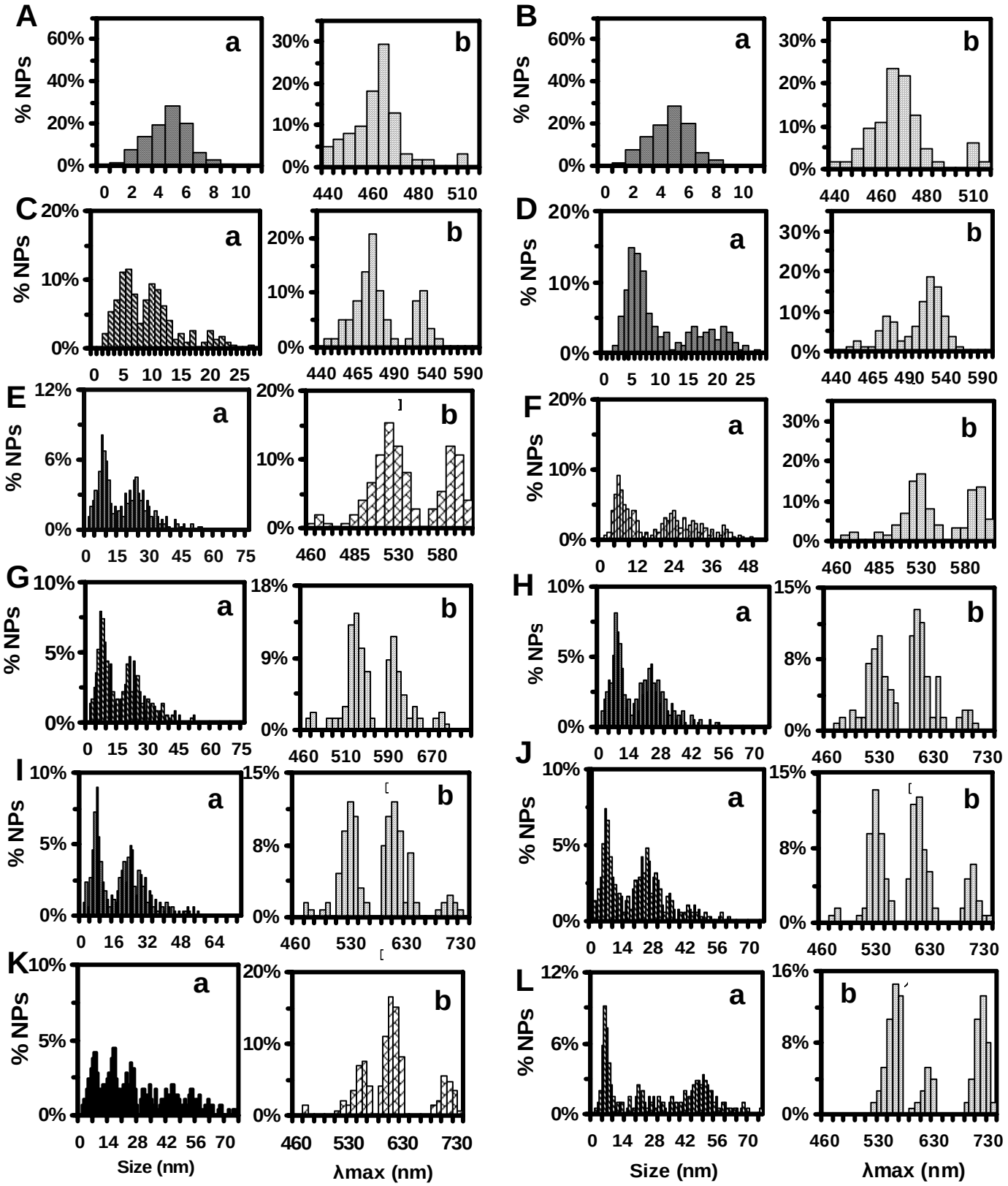

Figure 4

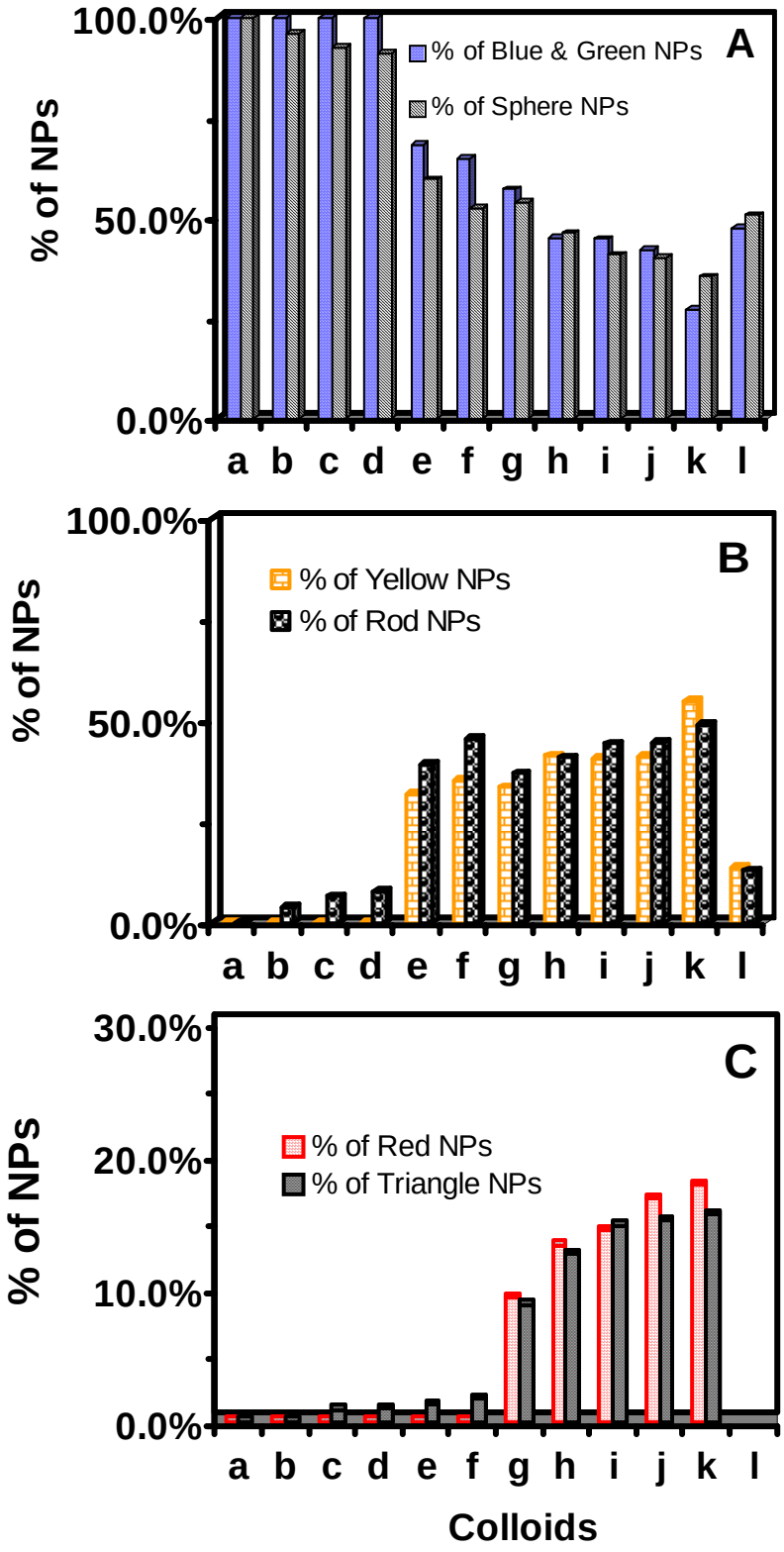
100.0%
50.0%
0.0%
% of NPs
% of Blue & Green NPs
% of Sphere NPs
A
a b c d e f g h i j k l
100.0%
50.0%
0.0%
% of NPs
% of Yellow NPs
% of Rod NPs
B
a b c d e f g h i j k l
30.0%
20.0%
10.0%
0.0%
% of NPs
% of Red NPs
% of Triangle NPs
C
a b c d e f g h i j k l
Colloids

Figure 5

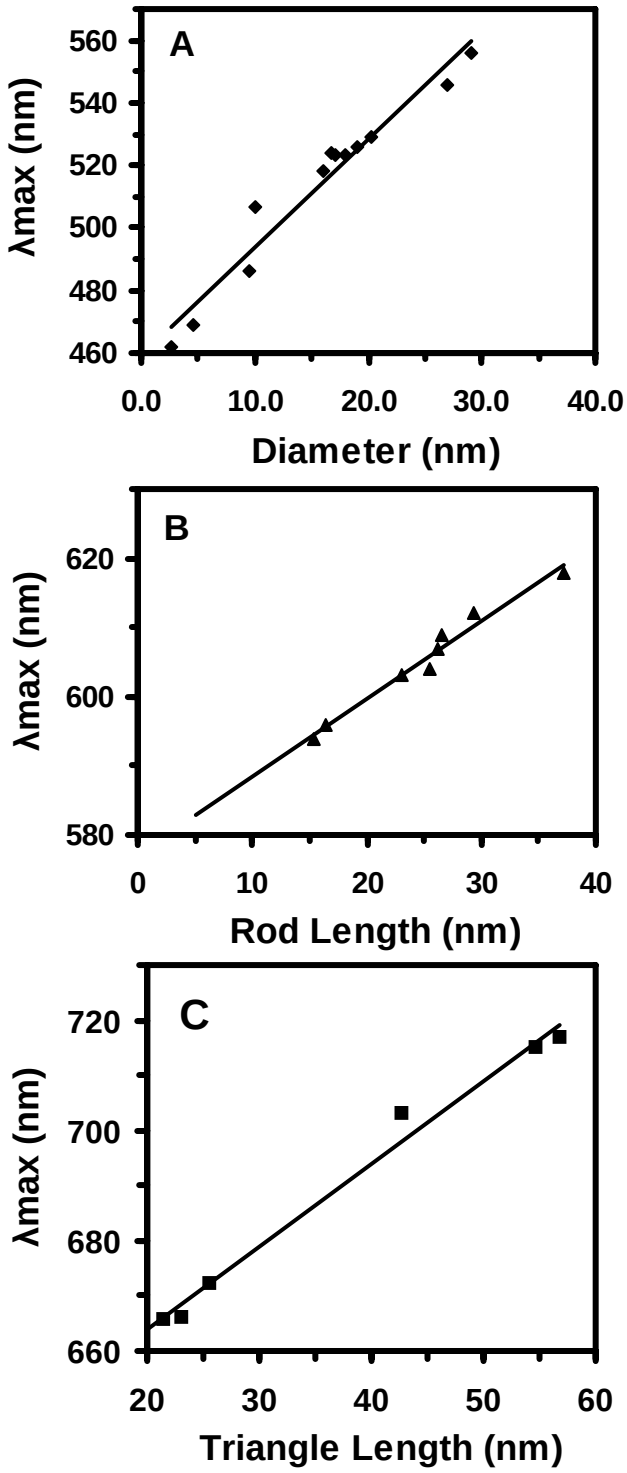
A
λmax (nm)
560
540
520
500
480
460
0.0
10.0
20.0
30.0
40.0
Diameter (nm)
B
λmax (nm)
620
600
580
0
10
20
30
40
Rod Length (nm)
C
λmax (nm)
720
700
680
660
20
30
40
50
60
Triangle Length (nm)

Figure 6

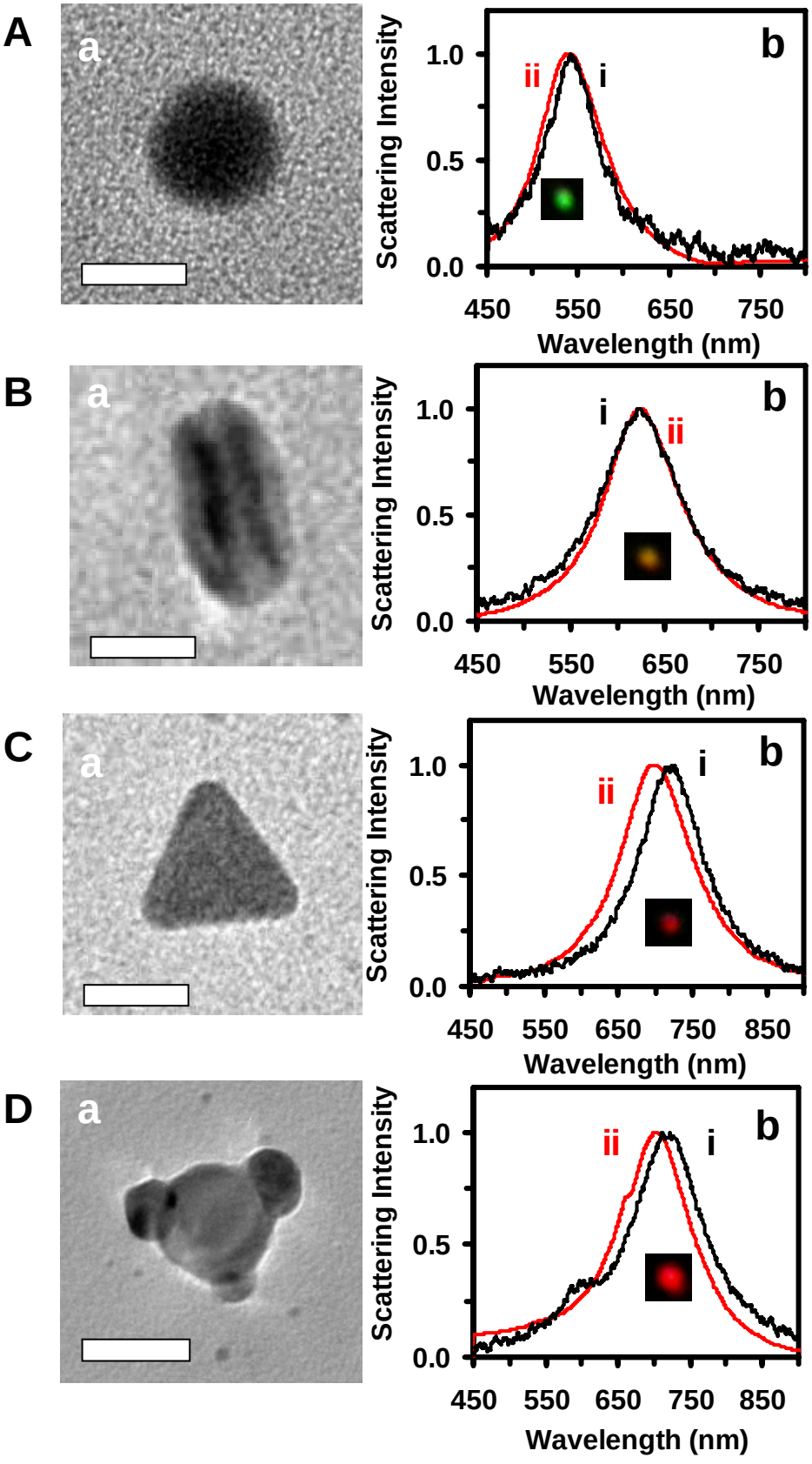
A
a
b
ii
i
Scattering Intensity
1.0
0.5
0.0
450
550
650
750
Wavelength (nm)
B
a
b
i
ii
Scattering Intensity
1.0
0.5
0.0
450
550
650
750
Wavelength (nm)
C
a
b
i
ii
Scattering Intensity
1.0
0.5
0.0
450
550
650
750
850
Wavelength (nm)
D
a
b
ii
i
Scattering Intensity
1.0
0.5
0.0
450
550
650
750
850
Wavelength (nm)

Table to Content (TOC)

Synthesis and Characterization of Tunable Rainbow Colored Colloidal Ag NPs at Single NP resolution